High-field magnetoresistance in $GaAs/Ga_{0.7}Al_{0.3}As$ heterojunctions arising from elastic and inelastic scattering

D. R. Leadley and R. J. Nicholas
Department of Physics, Clarendon Laboratory, Parks Road, Oxford, OX1 3PU, United Kingdom

W. Xu, F. M. Peeters, and J. T. Devreese
Departement Natuurkunde, Universiteit Antwerpen (UIA), Universiteitsplein 1, B-2610 Antwerpen, Belgium

J. Singleton* and J. A. A. J. Perenboom
High Field Magnet Laboratory, University of Nijmegen, Toerooiveld 1, NL-6525 ED, Nijmegen, The Netherlands

L. van Bockstal and F. Herlach
Laboratorium voor Lage Temperaturen en Hoge-Veldenfysika, KU Leuven, Celestijnenlaan 200 D, B-3001, Leuven, Belgium

C. T. Foxon
Department of Physics, The University, Nottingham, NG7 2RD, United Kingdom

J. J. Harris
Semiconductor Interdisciplinary Research Centre, Imperial College, London SW7 2BZ, United Kingdom
(Received 1 March 1993; revised manuscript received 20 May 1993)

In this paper we present measurements and calculations that explain the high-field magnetoresistance observed up to 30 T in $GaAs\text{-}Ga_xAl_{1-x}As$ heterojunctions over the temperature range 1.5–300 K. The scattering mechanisms that determine the mobility analogue $1/n_e e\rho_{xx}$ are compared at $B = 0$ and in high field, where it is found that the field and temperature dependence of the Landau-level broadening significantly influences the scattering. The calculations, based on the momentum balance equation, include all the scattering processes self-consistently in evaluation of both the density of states and resistivity. By this method we are able to obtain good agreement between experiment and theory, both at $B = 0$ and in high magnetic field.

I. INTRODUCTION

There are many physical properties that may be studied in two-dimensional electron systems of interest both from a fundamental viewpoint or with regard to device applications. In order to understand these properties it is necessary to have a clear picture of the various scattering mechanisms that limit the mobility μ of electrons in such structures. One of the most straightforward properties to measure is the Ohmic resistivity, from which μ may be extracted. In this work we are primarily concerned with the effect of a strong magnetic field B on the resistivity ρ_{xx} over a wide range of temperatures 4 K$< T <$ 300 K in $GaAs\text{-}Ga_xAl_{1-x}As$ single heterojunctions. While the mobility in the absence of magnetic field has received considerable attention,[1–4] studies of magnetoresistivity tend to have concentrated on regions of temperature and magnetic field where interesting oscillations occur, arising from the quantization of the electron energy. At low temperatures these are Shubnikov–de Haas oscillations and quantum Hall liquid effects, while at higher temperatures the oscillatory part of the magnetophonon effect has been concentrated on. Although anyone who has made transport measurements on high-mobility samples will recognize the strong increase in resistance with magnetic field, this has usually been regarded merely as an inconvenience and its origin was not explained.[5,6] Indeed classical theories of conduction in materials with one type of charge carrier predict no change of resistance in the high-magnetic-field region.[7] This study, a brief summary of which was recently presented,[8] is intended to shed some light on the effects of quantizing magnetic fields on the various scattering mechanisms influencing the resistance.

The mobility at $B = 0$ has been extensively studied in the past and a review of the various experiments and calculations prior to 1986 can be found in the paper of Hirakawa and Sakaki and the references therein.[1] Since then improvements in growth techniques have increased the measured mobilities,[3] some of the assumptions used in the theories have been questioned and refined,[4] and there has been much discussion over the values used for some of the fitting parameters, notably the deformation potential,[4,9] but the basic picture is really quite well understood.

The scattering processes that limit the mobility change according to the temperature and sample purity. At low temperatures the intrinsic mobility limit is due

0163-1829/93/48(8)/5457(12)/$06.00 ©1993 The American Physical Society

to acoustic-phonon scattering and in very-high-quality GaAs-$Ga_xAl_{1-x}As$ heterojunctions this is indeed observed as the dominant scattering mechanism with mobility values $\sim 10^3$ m^2/V s and $\mu \propto 1/T$ over the temperature range 1–80 K.[3,4] However, impurity scattering arising from background impurities in the GaAs or remote ionized donors in the $Ga_xAl_{1-x}As$ layer will always provide the ultimate limit on μ. As impurity scattering is only weakly dependent on temperature, samples with high impurity content exhibit a constant mobility over a large temperature range, while in purer samples acoustic-phonon scattering is relatively more important and μ continues to increase as the temperature is reduced. At higher temperatures optic-phonon scattering (OPS) dominates the mobility and by 300 K μ may be 500 times smaller than at 1 K.

Addition of a magnetic field has a profound effect on the resistivity by quantizing the electron energies into Landau levels (LL's) and so changing the density of states (DOS) available for scattering at a particular field or temperature. These LL's are often parametrized by a constant width Γ, but any scattering will increase Γ and so change the density of states. Hence, calculations of any observable properties have to be performed self-consistently and become quite involved when several scattering mechanisms need to be considered. To date the calculations of resistivity in magnetic field tend to be limited to cases where one scattering mechanism dominates the transport properties: either very low temperatures where only impurity scattering is considered and Shubnikov–de Haas oscillations are the major feature in ρ_{xx},[10,11] or high temperatures where OPS is most important. In the latter case magnetophonon resonances (MPR) are prominant and calculations have been made in a high-temperature approximation including either only LO-phonon scattering,[12] or treating each mechanism separately.[13] These high-temperature calculations invariably overestimate the sizes of MPR oscillations and do not account for a background magnetoresistance.[14]

This paper reports measurements of ρ_{xx} for a wide range of temperatures and magnetic fields in the limit of small filling factor $\nu(= n_eh/eB) \ll 1$, showing, amongst other things, a quasilinear increase of resistance with magnetic field; a remarkably constant value of ρ_{xx}, at fixed magnetic field, for a much larger temperature range than in zero field; and in some samples an unexpected decrease of ρ_{xx} at fixed magnetic field with increasing temperature in the region 10–80 K. These features are investigated in several GaAs-$Ga_xAl_{1-x}As$ heterojunctions with different carrier concentrations n_e and impurity densities to find the reason for these effects.

To explain the high-field magnetoresistance, self-consistent calculations of the various contributions to scattering are presented starting from a momentum-balance equation.[16] These show that the rather peculiar decrease in ρ_{xx} with temperature and its dependence on B are due to the variations in Γ and the effect this has on the scattering. The experimental data in zero magnetic field are accounted for using the carrier concentration and the zero-temperature, impurity-limited mobility $\mu^0_{\rm IMP}$ as the only sample-dependent parameters in the resistivity calculations. We are then able to calculate the high-field magnetoresistivity and reproduce the experimental results using the same sample parameters together with the ratio of the momentum to energy relaxation times γ.

The paper is organized as follows: the experimental results will be presented, followed by a development of the theory to include some analytic expressions for the mobility, valid under certain approximations; we will then discuss the agreement between experiment and theory, and finally draw some conclusions.

II. EXPERIMENTS

The magnetoresistance ρ_{xx} has been measured between 1 and 300 K in several high-quality GaAs-$Ga_xAl_{1-x}As$ heterojunctions. The measurements were performed over the full temperature range using a continuous-flow helium cryostat in a 9-T resistive magnet at the Clarendon Laboratory and at selected temperatures in the higher magnetic fields provided by pulsed fields of up to 36 T at KU Leuven and steady fields up to 30 T at the University of Nijmegen. An example of ρ_{xx} measured in the Nijmegen hybrid magnet is shown in Fig. 1 for sample G148 where MPR oscillations can be seen on top of a quasilinear background magnetoresistance. The results in each magnet system were the same but the rapid increase of resistance with magnetic field, especially in the low-density samples, made studies in pulsed magnetic fields more difficult due to the large RC time constants.

The samples were grown by molecular-beam epitaxy (MBE) at Philips Research Laboratories to a basic high-electron mobility transistor (HEMT) design[3] with carrier densities in the range $n_e = 0.16–3.2 \times 10^{15}$ m^{-2} as shown in Table I. In a given sample n_e could be increased by photoexcitation at low temperature and after illumination n_e remained constant on subsequent warming to 100 K, above which it relaxed rapidly to the original dark value. In all these heterojunctions only one electric subband is populated at low temperature, although there will be a small amount of thermal population of upper subbands at higher temperatures. There is no parallel

TABLE I. Sample parameters: n_e is measured at 4 K in the dark and $\mu^0_{\rm IMP}$ is the zero-temperature impurity-limited mobility. L_z is the width of the undoped $Ga_xAl_{1-x}As$ spacer layer.

Sample	L_z (Å)	n_e (10^{15} m^{-2})	$\mu^0_{\rm IMP}$ (m^2/V s)
G161	3200	0.16	9
G139	1600	0.30	28
G137	1600	0.31	33
G141	800	0.9	102
G156	800	1.0	76
G148	400	2.0	96
G104	200	2.8	40
G647	3200	0.15	30
G641	1600	0.25	170
G640	1200	0.51	310
G650	400	1.06	350

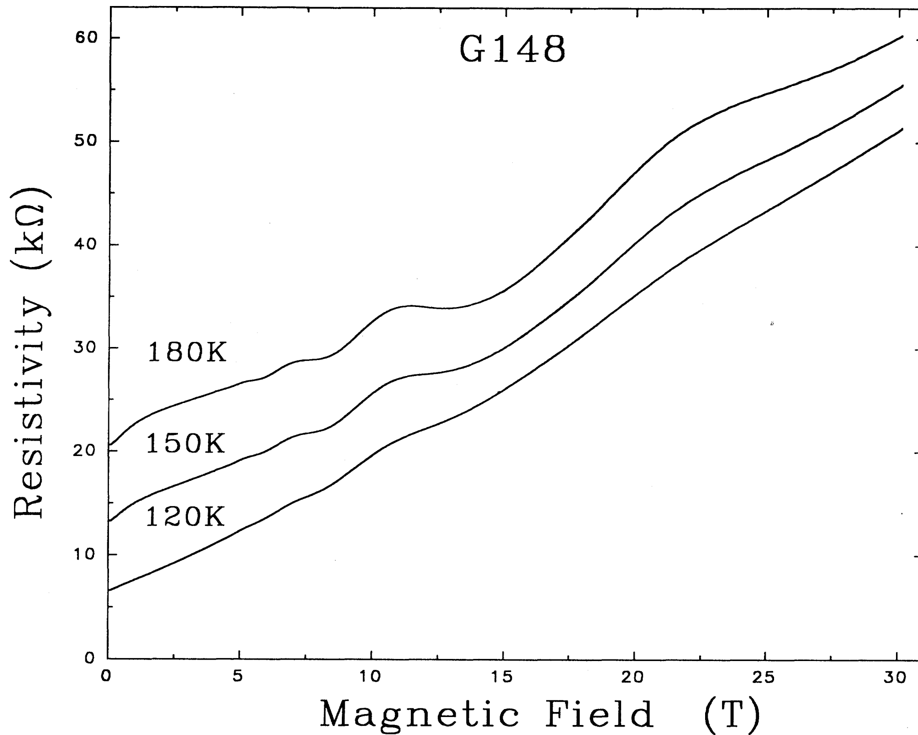

FIG. 1. Magnetoresistance ρ_{xx} of sample G148 at 120, 150, and 180 K showing a quasilinear magnetoresistance, with magnetophonon resonances superimposed.

conduction in the $Ga_xAl_{1-x}As$ layer of these samples at any temperature.

Illustrations of the temperature dependence of the mobility of GaAa-$Ga_xAl_{1-x}As$ heterojunctions in zero magnetic field are shown in Figs. 2 and 3. As this has already been studied intensively, we will not dwell extensively on our results but will only make a few points. At vanishingly small temperatures there will be no phonons present and, in the Ohmic region with which we are concerned, emission does not occur. Therefore, μ must be dominated by impurity scattering and the values quoted in Table I represent the maximum, impurity-limited mobil-

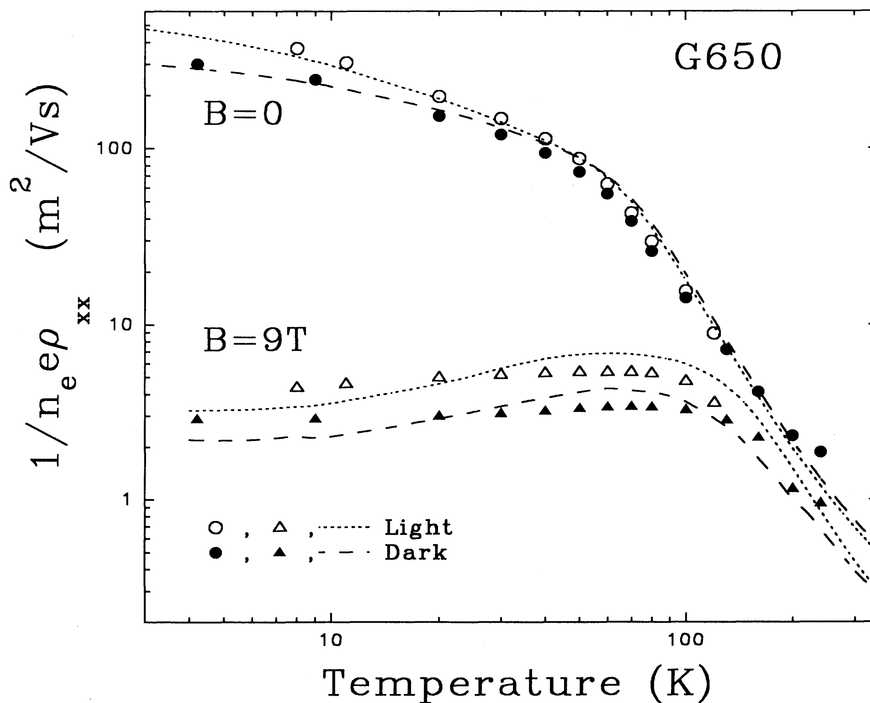

FIG. 2. Comparison of the experimental $1/n_e e\rho_{xx}$ for sample G650 (symbols) with calculations (lines) for $B = 0$ and 9 T. In the dark $n_e = 1.0 \times 10^{15}$ m^{-2} and $\mu^0_{IMP} = 350$ m^2/Vs increasing to $n_e = 1.7 \times 10^{15}$ m^{-2} and $\mu^0_{IMP} = 550$ m^2/Vs after illumination. We consider ten Landau levels and use $\gamma = 150$ in each case.

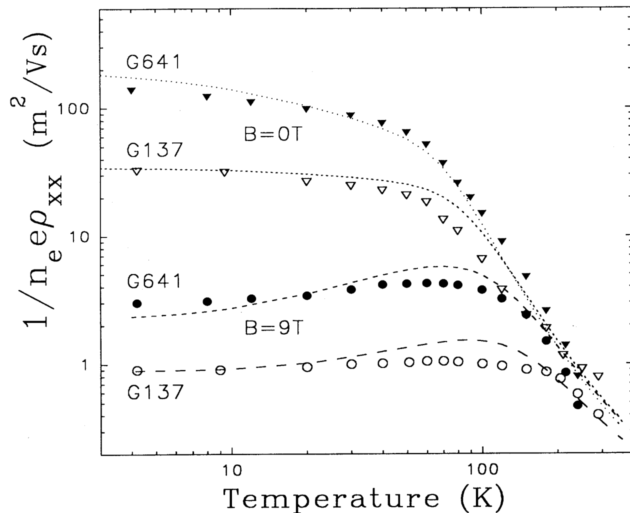

FIG. 3. Comparison of $1/n_e e\rho_{xx}$ between samples G137 (open symbols) and G641 (filled symbols) at $B = 0$ and 9 T. These samples have the same n_e but there is much less impurity scattering in G641. The lines show the calculations under conditions appropriate to these two samples, i.e., $n_e = 3.0 \times 10^{14}$ m^{-2}, $\mu^0_{\rm IMP} = 35$ m^2/V s, and $\gamma = 150$ for G137 and $n_e = 2.5 \times 10^{14}$ m^{-2}, $\mu^0_{\rm IMP} = 200$ m^2/V s, and $\gamma = 100$ for G641.

ity for the samples before photoexcitation. In the G600 series samples the mobility is dominated by acoustic-phonon scattering down to below 1 K so the values in the table are extrapolations to zero temperature.

The impurity scattering has been reduced in these G600 samples compared to the otherwise identical structures in the G100 series by the addition of a short-period superlattice in the buffer layer and by growing a wider, less heavily doped $Ga_xAl_{1-x}As$ donor layer. During MBE growth, impurities (especially carbon acceptors which are always present in semi-insulating substrates for compensation) tend to float on the surface of the GaAs, because at the MBE growth temperature Ga–C bonds are unstable with respect to Ga—As bond formation. However, when aluminum is introduced stable Al–C bonds are formed which thus trap the impurities at the first $Ga_xAl_{1-x}As$ interface. In standard HEMT material this is at the position of the two-dimensional electron gas (2DEG) and such impurities therefore seriously degrade the mobility. By growing a short-period GaAs/AlAs superlattice in the buffer layer the impurities migrating up from the substrate will be trapped well away from the 2DEG and this can result in a factor of 2 increase in mobility.[3]

The second improvement in mobility, which arises from reduced remote impurity scattering, can be understood by solving Poisson's equation for the structure. This shows that in equilibrium the doped $Ga_xAl_{1-x}As$ layer consists of three regions: a thin layer of ionized donors (typically as small as 10 Å thick) on the side nearest the 2DEG which provides the carriers in the 2DEG, a region of unionized donors, and a second thin ionized region which provides the band bending to the free surface. Remote impurity scattering can be reduced by growing a wider, less heavily doped layer, thus moving the second layer of charged impurities further from the 2DEG, and hence smoothing the potential seen by the electrons from the first ionized region.

As the temperature is increased the mobility decreases due to phonon scattering. Initially this is from acoustic phonons, but above 70 K OPS becomes dominant, causing a rapid increase in resistivity. By room temperature optic-phonon scattering is so strong that virtually no sample-dependent effects are observed and all the samples studied have the same value of $\mu = 0.8$ m^2/V s.

We now turn to the magnetic-field effects. At temperatures below 10 K Shubnikov–de Haas oscillations will feature strongly in the resistivity for fields below $\nu = 1$. However, the results presented here are all in low-electron-density samples at high magnetic fields so the filling factor is always very small. For example, in sample G137 all the electrons are in the lowest Landau level by 0.6 T (or 1.2 T if spin splitting is resolved) and above this field ρ_{xx} shows no Shubnikov–de Haas oscillations at low temperatures. (The temperature is never low enough for the fractional quantum Hall effect to be important.) At higher temperatures the electron energy distribution function will be much wider, allowing population of higher Landau levels once $kT \sim \hbar\omega_c$, at which point the filling factor ceases to be a meaningful quantity. At these temperatures the only oscillatory part of the resistivity will be due to magnetophonon resonance.

To compare the scattering mechanisms between samples and to investigate the effects of magnetic field we evaluated $1/n_e e\rho_{xx}$ at fixed magnetic fields (this is analogous to the zero-field mobility and would be expected to be equal to $\mu_{B=0}$ for a single carrier system with no magnetoresistance) over a wide temperature range. In each case n_e was measured from the Hall voltage to allow for changes in carrier concentration with temperature, which were negligible (< 1%) between 4 and 100 K in all cases, although an increase of typically 4×10^{14} m^{-2} was observed between 100 and 300 K in the lowest-density samples. A magnetic field of 9 T was chosen for the systematic comparison because it was near the maximum field obtainable from the Oxford magnet, in which the majority of the data was collected; $\nu \ll 1$ for all the samples; and it is near to a minimum of the magnetophonon resonance, so resonant optic-phonon scattering could be avoided.

Figure 2 compares $1/n_e e\rho_{xx}$ for sample G650 at $B = 0$ and 9 T in the dark and after illumination. For each of the samples in Table I we obtained qualitatively similar results. The figure shows that the magnetic field reduces the limiting value of $1/n_e e\rho_{xx}$ by a large factor at low temperature, but has a relatively small effect at high temperature, i.e., there is more magnetoresistance at low temperature than at high temperature. This suggests that the Landau quantization has a much greater effect on the quasielastic scattering mechanisms that dominate μ at low temperature than on OPS. Increasing the temperature at fixed magnetic field we see that $1/n_e e\rho_{xx}$ remains constant at low temperature, even in sample G650 for which μ in zero field still has a component due to

acoustic-phonon scattering below 1 K. $1/n_e e\rho_{xx}$ then increases slightly with temperature, in marked contrast to the $B = 0$ case, until the curve almost meets the $B = 0$ curve when the strong optic-phonon scattering becomes dominant, leading to a large reduction as in zero field. The temperature at which this cutoff occurs increases with increasing magnetic field.

In zero field the effect of photoexcitation is seen to have the greatest influence at the lowest temperature where impurity scattering plays the greatest part in determining μ. However, at 9 T the increase in $1/n_e e\rho_{xx}$ after illumination remains constant until 100 K, above which temperature the electron density starts to revert to its dark value. Both these facts suggest that impurity scattering may have a greater influence at higher temperatures in magnetic field, than at $B = 0$.

The comparison shown in Fig. 3 is between two samples with the same electron density but different impurity densities, G137 and G641, with both in the dark. On this logarithmic plot it can be seen that the ratio of μ at $B = 0$ to $1/n_e e\rho_{xx}$ at 9 T is similar for the two samples at low temperature, although $\mu^0_{\rm IMP}$ is five times greater in sample G641. This might suggest, as claimed in Ref. 6, that the magnetoresistance is some constant function for the material. However, this ratio is certainly not constant over all the samples we have studied at all temperatures, especially in the regions where $1/n_e e\rho_{xx}$ increases with temperature, and we will return to this point later. In the intermediate-temperature region a marked difference is observed with a much stronger increase in $1/n_e e\rho_{xx}$ seen for sample G641, which has the highest value of $\mu^0_{\rm IMP}$ and hence the narrowest Landau levels at low temperature.

In order to explain these effects it will be useful to have some model of how the different scattering processes interact in high magnetic field. So we will now discuss the calculations and will return to the interpretation in Sec. IV.

III. THEORY

A. The momentum balance equation

The calculation is based on the quantum-mechanical momentum-balance equation derived by Lei and coworkers,[15,16] which provides a much more tractable method of studying electron transport in quasi-two-dimensional (2D) systems under crossed **E** and **B** fields than by direct solution of the Boltzmann equation or use of the Kubo formula. The momentum balance equation is derived using a Green's-function approach to Thornber-Feynman theory[17] using statistical averaging over a density matrix satisfying Liouville's equation. Lei, Birman, and Ting previously used this approach to study the mobility in zero magnetic field[18] and we will follow their derivation but make certain approximations that allow us to arrive at explicit expressions for the various contributions to μ. We will then extend this framework to the high-magnetic-field case and contrast the two situations, with and without electron energies quantized into Landau levels. The calculation will be performed in the linear-response regime using the random-phase approximation, including scattering of electrons by impurities and acoustic and optic phonons. Electron-electron scattering will not be considered other than to allow the electron system to be described by a temperature T_e.

In this approach, the Hamiltonian and density matrix for the electrons may be written in center-of-mass and relative coordinates. The center-of-mass system then behaves as a single particle and only couples to the electrons in relative coordinates through electron-phonon and electron-impurity interactions. The statistics of the electrons in relative coordinates and of the phonons can be described by a density matrix taking the form of a product of the matrices for the separate systems and, in the absence of the interactions, we can use equilibrium distributions with characteristic temperatures T_e and T, respectively.

Considering 2D electrons and 3D phonons the momentum balance equation is

$$n_e e\mathbf{E} + n_e e(\mathbf{v}\times\mathbf{B}) + \sum_i \mathbf{F}_i(\mathbf{v}) = 0, \tag{1}$$

with $\mathbf{E}$ the electric field, $\mathbf{B}$ the magnetic field, $\mathbf{v} = (v_x, v_y)$ the electron center-of-mass velocity, and $\mathbf{F}_i(\mathbf{v})$ the frictional force induced by the ith scattering mechanism

$$\mathbf{F}_i(\mathbf{v}) = \sum_{\mathbf{Q},n',n} |U^i_{n'n}(\mathbf{Q},\omega_i)|^2\ \mathbf{q}\ \Pi_2(n',n,q,\omega_i+\mathbf{q}\cdot\mathbf{v})\ g_i, \tag{2}$$

where $\mathbf{Q} = (\mathbf{q}, q_z)$; $\mathbf{q} = (q_x, q_y)$; $\hbar\omega_i$ is the change of electron energy in the transition; $U^i_{n'n}(\mathbf{Q},\omega_i)$ is the interaction matrix element due to the ith scattering mechanism, summed over all the electron states n', n; g_i is a functional form related to the scattering mechanism, and $\Pi_2(n',n,q,\omega)$ is the imaginary part of

$$\Pi(n',n,\mathbf{q},\omega) = 2\sum_{\mathbf{k}} \frac{f[E_{n'}(\mathbf{k}+\mathbf{q})] - f[E_n(\mathbf{k})]}{\hbar\omega + E_{n'}(\mathbf{k}+\mathbf{q}) - E_n(\mathbf{k}) + i\delta}, \tag{3}$$

the Fourier transform of the electron density-density correlation function in relative coordinates, where $f(E)$ is the electron energy distribution function and $\delta \to 0^+$.

Two types of scattering need to be considered.

1. *Impurity scattering*

First, we consider elastic scattering from ionized impurities for which $g_i = 1$ and $\omega_i = 0$. In principle we should consider all the impurities in the sample, including both short-range scattering from the background impurities and long-range scattering from the remote ionized donors. This would require integrating over the density $n_{\rm imp}(z)$ and interaction matrix element $u^{\rm IMP}_{n'n}(\mathbf{q},z)$ of each plane of impurities. However, as we will take the mobility in the limit of $B \to 0, T \to 0$ as a single fitting

parameter in the model, we may describe the impurities by a single effective density N_I of δ-function scatterers throughout the sample. Thus the matrix element of Eq. (2) can be replaced by

$$\sum_{\mathbf{Q}} |U^{\rm IMP}_{n'n}(\mathbf{Q},0)|^2 = \sum_{\mathbf{q}} \int dz\; n_{\rm imp}(z) |u^{\rm IMP}_{n'n}(\mathbf{q},z)|^2 = N_I U_0^2 V^2 S_{n'n}, \quad (4)$$

where U_0 is the average impurity potential, V the sample volume, and $S_{n'n} = \int_{-\infty}^{\infty} dq_z \mathcal{G}^2_{n'n}(q_z)$. The form matrix $\mathcal{G}_{n'n}(q_z) = \langle n'|e^{iq_z z}|n\rangle$ takes account of the electron wave functions in the heterojunction potential for each electric subband n.

In samples with spacer layer thicknesses L_z of less than about 200 Å the effect of remote impurity scattering on the mobility would be comparable to that from background impurities[19] in zero field. However, the temperature dependence will be much the same for both types of impurity scattering, only entering through the temperature dependence of the screening length and the distribution of electron energies, so there will be no qualitative effect on our results by treating all the impurities together. Furthermore, this paper will be concentrating on the wider spacer layer samples. Again in high magnetic fields the electron cyclotron radius (~ 257 Å$/\sqrt{B}$) will be much smaller than the scale of fluctuations due to remote impurities ($\sim L_z$) so remote impurity scattering can be treated by the short-range delta-function approach described above.

The electrons are treated as being in equilibrium with the lattice so the linear-response regime is appropriate, i.e., $T_e = T$ and $|\mathbf{v}| \ll 1$, which makes the force terms of Eq. (2) linear in $\mathbf{v}$:

$$\mathbf{F}_{\rm IMP}(\mathbf{v}) = \mathbf{v}\; N_I U_0^2 V^2 \frac{\hbar}{4\pi} \times \sum_{n'n} S_{n'n} \int_0^\infty dq\; q^3 \times \left[\frac{\partial}{\partial(\hbar\omega)} \Pi_2(n',n,q,\omega)\right]_{\omega=0}. \quad (5)$$

2. Phonon scattering

Next we consider phonon scattering for which $g_i = 2\{N_Q(\hbar\omega_Q/k_BT) - N_Q[\hbar(\omega_Q + \mathbf{q}\cdot\mathbf{v})/k_BT_e]\}$ where $N_Q(x) = 1/(e^x - 1)$ is the Bose function and ω_Q is the phonon frequency. The first term represents phonon absorption and the second phonon emission. We will consider separately the cases of inelastic LO-phonon scattering and quasielastic acoustic-phonon scattering.

(i) For polar-optic-phonon scattering there is only one frequency $\omega_Q = \omega_{\rm LO}$ and $N_Q = N_0 = 1/(e^{\hbar\omega_{\rm LO}/k_BT} - 1)$, so in the linear-response regime $g_i \approx 2N_0(1+N_0)\mathbf{q}\cdot\mathbf{v}/k_BT$, and the matrix element becomes

$$\sum_{q_z} |U^{\rm LO}_{n'n}(Q)|^2 = 2\alpha L_0 (\hbar\omega_{\rm LO})^2 X_{n'n}(q), \quad (6)$$

where α is the electron LO-phonon coupling constant, $L_0 = (\hbar/2m^*\omega_{\rm LO})^{1/2}$ is the polaron radius, $\hbar\omega_{\rm LO}$ the LO-phonon energy, and $X_{n'n}(q) = \int_{-\infty}^{\infty} dq_z\, |\mathcal{G}_{n'n}(q_z)|^2/(q^2 + q_z^2)$. For GaAs we take $\alpha = 0.068, L_0 = 39.5$ Å, and $\hbar\omega_{\rm LO} = 36.5$ meV.

When $|v| \ll 1$ the force term becomes

$$\mathbf{F}_{\rm LO}(\mathbf{v}) = \mathbf{v}\; \frac{\alpha L_0 \hbar(\hbar\omega_{\rm LO})^2 N_0(1+N_0)}{\pi k_B T} \times \sum_{n',n} \int_0^\infty dq\; q^3 X_{n'n}(q) \Pi_2(n',n,q,\omega_{\rm LO}). \quad (7)$$

(ii) For acoustic-phonon scattering via the deformation potential (DPA phonons) $\omega_Q = u_{sl}Q$ and

$$|U^{\rm DPA}_{n'n}(Q)|^2 = \frac{\hbar E_D^2 Q}{2\rho u_{sl}} \mathcal{G}^2_{n'n}(q_z), \quad (8)$$

with u_{sl} the longitudinal sound velocity, ρ the density of the material, and E_D the deformation-potential-energy constant. Under the elastic-scattering approximation, i.e., $\omega_Q \ll 1$, $N_Q \simeq N_Q + 1 \simeq k_BT/\hbar u_{sl}Q$ and the force term for DPA scattering becomes

$$\mathbf{F}_{\rm DPA}(\mathbf{v}) = \mathbf{v}\; \frac{E_D^2}{\rho u_{sl}^2} \frac{\hbar k_B T}{8\pi^2} \times \sum_{n'n} S_{n'n} \int_0^\infty dq\; q^3 \times \left[\frac{\partial}{\partial(\hbar\omega)} \Pi_2(n',n,q,\omega)\right]_{\omega=0}. \quad (9)$$

Tanatar, Singh, and MacDonald[20] have studied the effects of including inelastic DPA scattering and impurity scattering self-consistently and find additional peaks in the DOS when E_F is away from the center of the Landau levels and at higher temperatures some transfer of DOS from the center to the wings of the LL's. However, these are rather small effects ($< 10\%$) at low temperature and will be swamped by optic-phonon broadening at high temperature. Above 4 K the available acoustic-phonon energies will be small compared to k_BT so the broadening will mostly be due to the spread of the electron energy distribution function and the elastic approach is justified.

Acoustic-phonon scattering via piezoelectric coupling could also be considered, but this will have a similar temperature and magnetic-field dependence to DPA scattering and so is not included separately. It could be accounted for by changing the value used for E_D and its neglect will not qualitatively affect the results.

For GaAs we take the deformation potential $E_D = 10$ eV, the material density as 5370 kg m^{-3}, and the longitudinal-acoustic velocity as 5.3×10^7 m s^{-1}.

Comparing Eqs. (5) and (9) we notice that elastic scat-

tering from DPA phonons has the same functional form as scattering from the background δ-like impurities and so will have a similar effect on the magnetotransport. However the temperature and electron-density dependencies will be different.

To calculate $S_{n'n}$ and $X_{n'n}(q)$ it is necessary to know the z dependence of the electron wave functions. For these low-electron-density $GaAs/Al_xGa_{1-x}As$ heterojunctions ($n_e < 5 \times 10^{15}$ m^{-2}), we may assume that only the lowest electric subband $n' = n = 0$ is occupied. Then applying the Fang-Howard self-consistent approximation to model the heterojunction,[21] we have

$$S_{00} = \frac{3\pi b}{8} \tag{10}$$

and

$$\frac{q^2}{q^2 + q_z^2} \simeq \frac{1}{1 + b^2 L_0^2/3}, \tag{11}$$

which gives

$$X_{00}(q) \simeq \frac{3\pi b}{8q^2} \frac{1}{1 + b^2 L_0^2/3}, \tag{12}$$

where $b = [\frac{48\pi m^* e^2}{\kappa\hbar^2}(N_{\rm depl} + \frac{11}{32}n_e)]^{1/3}$ defines the potential well, with κ the static dielectric constant of the material (in SI units $\kappa = 4\pi\epsilon_0\epsilon_r$), and $N_{\rm depl}$ the depletion charge density. For this material $N_{\rm depl} \sim 10^{13}$ m^{-2}.[22]

Thus the force terms in the momentum balance equation appropriate for the linear-response regime when only the lowest electric subband is occupied with electrons are

$$\begin{aligned}
\mathbf{F}_{\rm IMP}(\mathbf{v}) &= \mathbf{v}\; N_I U_0^2 V^2 \frac{3b\hbar}{32}\, \mathcal{G}_0, \\
\mathbf{F}_{\rm DPA}(\mathbf{v}) &= \mathbf{v}\; \frac{E_D^2}{\rho u_{sl}^2} \frac{3b\hbar}{64\pi}\, k_B T\, \mathcal{G}_0, \\
\mathbf{F}_{\rm LO}(\mathbf{v}) &= \mathbf{v}\; \frac{3b\hbar\alpha L_0 (\hbar\omega_{\rm LO})^2 N_0 (1 + N_0)}{8(1 + b^2 L_0^2/3) k_B T}\, \mathcal{G}_1,
\end{aligned} \tag{13}$$

with $\mathcal{G}_0 = \int_0^\infty dq\; q^3 [\frac{\partial}{\partial(\hbar\omega)} \Pi_2(q,\omega)]_{\omega=0}$ and $\mathcal{G}_1 = \int_0^\infty dq\; q\; \Pi_2(q, \omega_{\rm LO})$.

Finally we must calculate Π_2 taking into account the variation with temperature and magnetic field of the electron energy distribution.

B. Zero-field mobility

In the absence of a magnetic field

$$\Pi_2(q,\omega) = -\frac{(2m^*)^{3/2}}{4\pi\hbar^3 q} \int_0^\infty \frac{dE}{\sqrt{E}} [f(E + \varepsilon - \hbar\omega) - f(E + \varepsilon)], \tag{14}$$

where $\varepsilon = \varepsilon_0 + (\epsilon_q + \hbar\omega)^2/4\epsilon_q$ with ε_0 the energy of the lowest electric subband and $\epsilon_q = \hbar^2 q^2/2m^*$. In calculating $\mathcal{G}_0$ for impurity and DPA scattering, which are of importance for low temperatures, the energy distribution is described by the Fermi-Dirac function $f(E) = 1/[e^{(E-E_F)/k_B T} + 1]$ with E_F the Fermi energy. For $\mathcal{G}_1$, appropriate to LO-phonon scattering which dominates at high temperature ($T > 50$ K), a Maxwellian distribution $f(E) = ce^{E/k_B T}$ is used. In each case E_F and c are determined by conserving the number of electrons. The results are $\mathcal{G}_0 = 4\pi m^{*2}\hbar^{-4} n_e$ and $\mathcal{G}_1 = \pi m^* \hbar^{-2} (N_0 + 1)^{-1} n_e$.

The mobility can then be calculated directly from the momentum balance equation using its definition of drift velocity per unit applied field:

$$\frac{1}{\mu} = \frac{\mathbf{E}\cdot\mathbf{v}}{v^2} = \frac{1}{n_e e} \sum_i \frac{\mathbf{F}_i(\mathbf{v})\cdot\mathbf{v}}{v^2}. \tag{15}$$

Since the $\mathbf{F}_i$ are linear in $\mathbf{v}$ and not coupled, we can write

$$\frac{1}{\mu} = \frac{1}{\mu_{\rm IMP}^0} + \frac{1}{\mu_{\rm DPA}} + \frac{1}{\mu_{\rm LO}}, \tag{16}$$

and the contributions from each scattering mechanism can be found from Eq. (13).

The expression

$$\frac{1}{\mu_{\rm IMP}^0} = N_I U_0^2 V^2 \frac{3\pi b m^{*2}}{8\hbar^3 e} \tag{17}$$

is the impurity contribution, which is temperature independent. Since the impurity distribution is not well known, the low-temperature limit of the experimental results will be used to determine $\mu_{\rm IMP}^0$ for each sample. Applying the static Debye screening approach, we found that the impurity scattering potential constant $U_0 \sim n_e^{-1/2}$ and, consequently, the electron density dependence of the mobility at zero temperature and in zero magnetic field is $\mu_{\rm IMP}^0 \sim n_e b^{-1}$, for a fixed impurity density. In practice $\mu_{\rm IMP}^0$ does not continue to increase with n_e since higher-density heterojunctions have narrower spacer layers and remote impurity scattering then becomes important and reduces μ.

The acoustic-phonon-scattering contribution to the inverse mobility is

$$\frac{1}{\mu_{\rm DPA}} = \frac{E_D^2}{\rho u_{sl}^2} \frac{3bm^{*2}}{16\hbar^3 e} k_B T, \tag{18}$$

which is seen to only depend on n_e through b and varies linearly with temperature. The LO-phonon contribution is

$$\frac{1}{\mu_{\rm LO}} = \frac{3\pi\alpha b\hbar^2\omega_{\rm LO}}{16eL_0(1 + b^2L_0^2/3)} \frac{N_0}{k_B T} I(T), \tag{19}$$

where $I(T) = 1$ in the momentum-balance-equation approach. A much more rapid temperature dependence largely determined by N_0 is found and again the result exhibits only a weak electron-density dependence. It was pointed out by several authors[23] that the momentum balance equation may not give the correct result in the zero-magnetic-field limit. Indeed if we do the same calculation using the Kubo formula in the relaxation-time approximation we obtain Eq. (19) with

$$I(T) = \frac{2}{\beta_0}\left(\frac{e^{\beta_0} + 1}{e^{\beta_0} - \beta_0}\right), \tag{20}$$

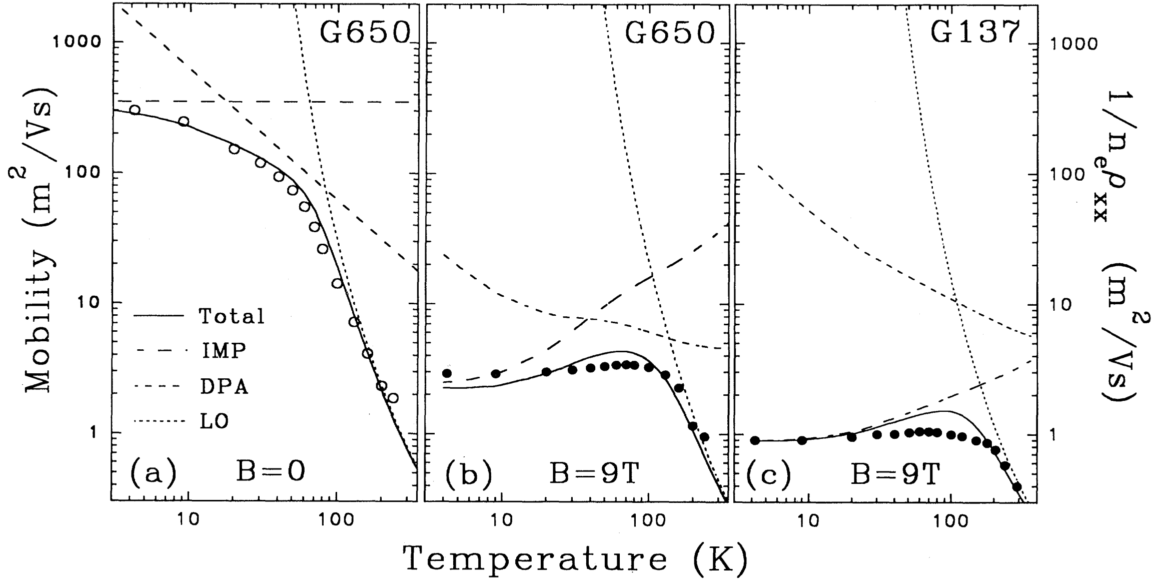

FIG. 4. Separate contributions of impurity, DPA- and LO-phonon scattering to $1/n_e e\rho_{xx}$. (a) For sample G650 at $B = 0$, (b) G650 at 9 T, and (c) G137 at 9 T. The solid line represents the total and the circles are the experimental data. The parameters used in the calculations are listed for Figs. 2 and 3. Notice how the acoustic-phonon contribution in high field changes for the two samples due to their different impurity concentrations.

where $\beta_0 = \hbar\omega_{\rm LO}/k_BT$. We know[24] that in three-dimensions such an approach gives the correct result for the mobility limited by optic phonons. In the following we will include this factor in our calculation which will reduce the mobility $1/n_e e\rho_{xx}$ in the temperature range where optic phonons are the dominant scattering mechanism. For impurity scattering and scattering with acoustic phonons no such factor has to be included.

The numerical results of the contribution each type of scattering makes to μ can be seen in Fig. 4(a) for sample G650. If $\mu^0_{\rm IMP}$ is used as a parameter to fit the experimental results over the full temperature range, a value of 350 m^2/V s is found, in agreement with the low-temperature measurements.

C. High magnetic field

In a high magnetic field the $\mathbf{F}_i$ are no longer independent of each other as Π_2 now varies with the *total* amount of scattering present. Following Cai, Lei, and Ting,[16] the imaginary part of the electron density-density correlation function, neglecting electron-electron screening effects is

$$\Pi_2(q,\omega) = \frac{1}{2\pi l^2}\sum_{N'N} C_{N'N}(l^2q^2/2)\,\Pi_2(N',N,\omega), \quad (21)$$

where $l = (\hbar/eB)^{1/2}$ is the magnetic length, N' and N are initial and final Landau-level indices,

$$C_{N,N+J}(y) = \frac{N!}{(N+J)!}y^J e^{-y}[L_N^J(y)]^2, \quad (22)$$

with $L_N^J(y)$ the associated Laguerre polynomials, and

$$\Pi_2(N',N,\omega) = -\frac{2}{\pi}\int_{-\infty}^{\infty} dE[f(E) - f(E+\hbar\omega)] \times {\rm Im}G_{N'}(E+\hbar\omega){\rm Im}G_N(E). \quad (23)$$

${\rm Im}G_N(E)$ is the imaginary part of the Green's function for the Nth Landau level, which is proportional to the density of states $D_N(E) = (2/\pi^2l^2){\rm Im}G_N(E)$. The conservation of electron number, used to determine E_F at each T, B now requires a summation over all the Landau levels:

$$n_e = -\frac{1}{\pi^2l^2}\sum_{N=0}^{\infty}\int_{-\infty}^{\infty} dE\, f(E){\rm Im}G_N(E). \quad (24)$$

With $\mathbf{B}$ perpendicular to the 2DEG the magnetoresistivities can be calculated from the momentum balance equation in high magnetic field by taking the dot and cross products respectively with $\mathbf{v}$:

$$n_e e\rho_{xx} = \sum_i \frac{\mathbf{F}_i\cdot\mathbf{v}}{v^2} = BA \quad \text{and} \quad n_e e\rho_{xy} = B, \quad (25)$$

where we choose to define the scalar

$$A = A_{\rm IMP} + A_{\rm DPA} + A_{\rm LO} \quad (26)$$

for convenience. Comparing this with Eq. (16) shows how $1/n_e e\rho_{xx}$ can be regarded as the high-field analogue of the mobility defined at $B = 0$. Substitution for the high-field expressions of Π_2 in the force terms yields

$$A_{\mathrm{IMP}} = \frac{1}{\mu^0_{\mathrm{IMP}}} \frac{e\hbar\omega_c^2}{\pi^3 n_e} \sum_{N',N} (N' + N + 1)\mathcal{F}^0_{N'N},$$

$$A_{\mathrm{DPA}} = \frac{E_D^2}{\rho u_{sl}^2} \frac{3bm^{*2}k_BT\omega_c^2}{32\pi^3\hbar^2 n_e} \sum_{N',N} (N' + N + 1)\mathcal{F}^0_{N'N}, \tag{27}$$

$$A_{\mathrm{LO}} = \frac{3\alpha b N_0(1+N_0)\hbar\omega_{\mathrm{LO}}\omega_c}{16\pi^2 n_e L_0(1 + b^2L_0^2/3)k_BT} I(T) \sum_{N',N} \mathcal{F}^1_{N'N},$$

where

$$\mathcal{F}^0_{N'N} = -\int_{-\infty}^{\infty} dE \, \frac{\partial f(E)}{\partial E} \mathrm{Im}G_{N'}(E)\mathrm{Im}G_N(E),$$

$$\mathcal{F}^1_{N'N} = \int_{-\infty}^{\infty} dE \, [f(E) - f(E + \hbar\omega_{\mathrm{LO}})] \times \mathrm{Im}G_{N'}(E + \hbar\omega_{\mathrm{LO}})\mathrm{Im}G_N(E). \tag{28}$$

Equation (25) is not identical to Matthiessen's rule since the contributions to the resistivity from each scattering mechanism are not independent. This is because the energy averaging in Eq. (28) is over Green's functions which include the effects of *all* the scattering mechanisms.

In order to calculate the magnetoresistivity we still need the imaginary part of the Green's functions for each Landau level, i.e., we have to solve the problem of the Landau-level broadening induced by the interaction of the electrons with the different scattering mechanisms.

In the presence of a high magnetic field, the Green's function for the Nth Landau level is given by

$$G_N(E) = \frac{1}{E - E_N - \Sigma_N(E)}, \tag{29}$$

where $E_N = (N + 1/2)\hbar\omega_c$ is the energy of the Nth Landau level with the self-energy

$$\Sigma_N(E) = \Delta_N(E) - i\Gamma_N(E)/2. \tag{30}$$

The real part $\Delta_N(E)$ results in an energy shift and the imaginary part $\Gamma_N(E)/2$ determines the width of the Landau level.

Previous calculations have used a high-temperature approximation[13] to find the self-energy in which contributions to Γ_N are calculated independently for each scattering process but then added to give a total broadening which is used to calculate the resistivity. However, each type of scattering will influence the DOS available for the other mechanisms so we will perform the complete calculation self-consistently.

The self-energy is calculated including scattering with (i) impurities, (ii) DPA phonons, and (iii) LO phonons. For the quasielastic scattering with impurities and DPA phonons the well-known[10] lowest self-consistent Born approximation (SCBA) is applied, while for LO-phonon scattering the one-phonon self-energy[25] is used. This leads to the following result:

$$\Sigma_N(E) = 2\sum_{N',\mathbf{q}} C_{N'N}\left(\frac{l^2q^2}{2}\right)\{|U^{\mathrm{IMP}}(q)|^2 G_{N'}(E) + |U^{\mathrm{DPA}}(q)|^2 G_{N'}(E) + |U^{\mathrm{LO}}(q)|^2\,[N_0 + f_{N'}(E)]G_{N'}(E + \hbar\omega_{\mathrm{LO}}) + |U^{\mathrm{LO}}(q)|^2\,[N_0 + 1 - f_{N'}(E)]G_{N'}(E - \hbar\omega_{\mathrm{LO}})\}, \tag{31}$$

where $f_N(E) = 1/(e^{(E-E_N)/k_BT} + 1)$ is the distribution function centered on the Nth Landau level and a factor of 2 is included for spin degeneracy. In this calculation we do not make the approximation of Eq. (11) for the LO-phonon contribution as this would preclude intra-LL scattering.

Introducing the square of the interaction matrix element for the different scattering mechanisms $U^i(q)$, we obtain

$$\Sigma_N(E) = \sum_{N'} \{(\mathcal{W}_{\mathrm{IMP}} + \mathcal{W}_{\mathrm{DPA}})G_{N'}(E) + \mathcal{W}_{\mathrm{LO}}[N_0 + f_{N'}(E)]G_{N'}(E + \hbar\omega_{\mathrm{LO}}) + \mathcal{W}_{\mathrm{LO}}[N_0 + 1 - f_{N'}(E)] \times G_{N'}(E - \hbar\omega_{\mathrm{LO}})\}, \tag{32}$$

with

$$\mathcal{W}_{\mathrm{IMP}} = \frac{\gamma}{\mu^0_{\mathrm{IMP}}} \frac{e\hbar^2}{\pi m^*}\omega_c, \tag{33}$$

$$\mathcal{W}_{\mathrm{DPA}} = \frac{E_D^2}{\rho u_{sl}^2} \frac{3bm^* k_BT}{64\pi\hbar}\omega_c, \tag{34}$$

$$\mathcal{W}_{\mathrm{LO}} = \frac{\alpha L_0 b(\hbar\omega_{LO})^2}{8}\mathcal{I}_{N'N}, \tag{35}$$

where

$$\mathcal{I}_{N'N} = \int_0^{\infty} dx \frac{8a^2 + 9ax + 3x^2}{(x+a)^3} C_{N'N}(x^2), \quad a = \frac{bl}{\sqrt{2}}.$$

The present approach leads to the well-known result of Ando,[10] $\Gamma \sim \sqrt{B}$, if we assume that the relevant energies are close to the center of the LL and if only elastic impurity scattering is included. At this point it is important to recognize that there are two scattering times to consider: the energy relaxation time (or quantum lifetime) τ_q, which determines the Landau-level broadening, and the momentum relaxation time (or classical lifetime) τ_c, which determines the mobility. For phonon scattering $\tau_q = \tau_c$ and this is also true for scattering from the delta-scatters used in the model appropriate for background impurities. However, for long-range impurity scattering from remote ionized donors $\tau_q \ll \tau_c$. We will correct

for this by taking a different effective impurity density [we use $\gamma = \tau_c/\tau_q$ in Eq. (33) as a fitting parameter] in the calculation of the Landau-level width from that used to calculate the resistivity. In our previous work[8] we omitted this factor and made the high-temperature approximation for the LO-phonon contribution yet were still able to obtain a reasonable fit to the data, but there were greater deviations in the intermediate-temperature region where the impurity contribution was underestimated.

Considering the center of each Landau level with $E = E_N$, Eqs. (29) and (32) were solved iteratively for the self-energy, which we assume not to vary within a given LL and define $\Gamma_N = \Gamma_N(E_N)$ and $\Delta_N = \Delta_N(E_N)$. In our theoretical calculation of the resistivity we take for the imaginary part of the Green's function

$$\mathrm{Im}G_N(E) = -\frac{2}{\Gamma_N}\mathrm{Re}\left[1 - \left(\frac{E - \Delta_N - E_N}{\Gamma_N}\right)^2\right], \quad (36)$$

where the LL width Γ_N is determined by the above self-consistent calculation and has different temperature and magnetic-field dependencies for each N.

By comparison, in the high-temperature approximation the LL width from each scattering process Γ_i is calculated separately and the total Landau-level width found from $\Gamma_N^2 = \Gamma_{\mathrm{IMP}}^2 + \Gamma_{\mathrm{DPA}}^2 + \Gamma_{\mathrm{LO}}^2$. We find that for each scattering process $\Gamma_i^2 = 8\mathcal{W}_i$ and so inspection of Eqs. (33), etc. shows that all the Landau levels would have the same shape and width with a field dependence $\Gamma \propto \sqrt{B}$. Clearly there is a large difference between the full calculation of Eq. (32) and this approximation.

The calculated contribution to $1/n_e e\rho_{xx}$ from each scattering mechanism is shown in Fig. 4(b) for sample G650. The total is also shown by the lines in Fig. 2 where it should be noted that the value of μ_{IMP}^0 fitted to the zero-field, dark data and γ are the only parameters. Therefore the 9-T calculations in the dark and after illumination represent very good agreement between experiment and theory. The values of the fitting parameters are very similar to the experimentally determined values shown in Table I. Similar results and agreement can be obtained for the other samples using μ_{IMP}^0, n_e, and γ as the only sample-dependent parameters. Figure 4(c) compares the case for sample G137 which has a much greater impurity density. Again the calculation shows a pronounced increase in $1/n_e e\rho_{xx}$ in the intermediate-temperature region due to changes in the LL width. For sample G137 this is almost exclusively due to a reduction in impurity scattering, whereas the data for sample G650 shows both the elastic-scattering processes behaving in the same manner.

For the calculations at 9 T we have included ten Landau levels, corresponding to an energy range of 155 meV, i.e., $\gg \hbar\omega_{\mathrm{LO}}$. At lower fields more levels must be considered to correctly account for inelastic LO-phonon scattering. This considerably increases the CPU time required, but otherwise the calculated $1/n_e e\rho_{xx}$ overestimates the experimental data at high temperatures and does not show the required increase at intermediate temperatures where OPS has a significant effect on Γ.

IV. DISCUSSION

We are now in position to explain the magnetoresistance seen in Fig. 1, i.e., the field dependence of $1/n_e e\rho_{xx}$. This is basically a result of changes in the density of states in the Landau levels as the field changes. Very simply the total number of states in each LL is eB/h and if the width of each level increases like $\sqrt{B}$ then at energies near the center of the LL, where most of the conduction originates, the DOS will increase with magnetic field like $\sqrt{B}$. The probability of an intralevel scattering event will depend on the product of initial and final states and so increases linearly in magnetic field. Thus we have a linear magnetoresistance. However, as closer inspection of the calculations reveals, there are energy integrals to consider which will change as the DOS changes and so a strictly linear change is not expected.

By treating $1/n_e e\rho_{xx}$ as a mobility and extracting a scattering time from the relationship $\mu = e\tau/m^*$, we find that τ decreases rapidly when a magnetic field is applied, i.e., the width of the lowest Landau level is changing with magnetic field. This is quite different from the situation at low temperature and low magnetic fields where a constant τ_q is used to describe the damping of Shubnikov–de Haas oscillations. This τ_q has been shown not to vary with magnetic field by measuring the amplitudes of a large number of oscillations, provided the oscillations are only a small perturbation on the resistivity, which implies a constant Landau-level width within this restricted field range. The present calculations show that while τ_q may be the quantity of interest when there are many overlapping Landau levels, this can not be extended to the high-field region. The interchange of these very different quantities may be responsible for considerable confusion in calculations of magnetophonon resonance at high temperature and high magnetic field.[14]

Rötger *et al.*[6] made measurements of ρ_{xx} on a set of heterojunctions and found that the magnetoresistance was approximately linear at temperatures where OPS was not important. They found further that by expressing $\rho_{xx} = \rho_0 + \alpha B + \beta B^2$ the linear coefficient [which they called α and which is the same as our A in Eq. (25)] was constant for all their samples below 30K and took a value of 0.07. At higher temperature α increased but by different amounts for each sample. However, by a suitable normalization they were able to recover the sample-independent relationship $\alpha(T) = 0.07\sqrt{\mu/\mu(T)}$ and went on to speculate what this might mean.

It was stated earlier that, for impurity scattering only, the equations show $\Gamma \propto \sqrt{B}$ and in the limit of very small Γ and ignoring the energy averaging, this makes $\mathcal{F}_{N'N}^0 \sim \Gamma^{-4} \sim B^{-2}$ and hence the elastic-scattering mechanisms could give rise to a linear increase in ρ_{xx} with magnetic field. However, the energy averaging and the influence of other scattering mechanisms on Γ will mean that the magnetoresistance will not in practice be strictly linear. Under the same approximation with $\Gamma^2 = \mathcal{W}_{\mathrm{IMP}}$ and $A = A_{\mathrm{IMP}}$ our calculations do show A is independent of the impurity density (but not of γ) and so could be sample independent, but again the added complications of other scattering affecting Γ and energy averaging sug-

gest this will not always be true, especially if the relative contribution from remote impurity scattering, and hence γ changes.

Closer inspection of the diagrams in Ref. 6 reveals quite a scatter of data points, but the error bars given make their interpretation plausible. We have performed a similar analysis on our data, fitting ρ_{xx} to a polynomial in B up to 30 T and finding the background magnetoresistance is again predominantly linear, with small amounts of higher terms. However, the value of A is extremely sample dependent, varying by over an order of magnitude as seen in Fig. 5. There is also a large dip for some samples associated with the increase in $1/n_e e\rho_{xx}$ at intermediate temperatures. We are therefore not able to extend this "universal" relationship and tend towards the conclusion that the result of Ref. 6 was due to a rather fortuitous choice of heterojunctions and that there is no universality about the number 0.07.

As Figs. 2–4 show the agreement between theory and experiment is remarkably good. The interesting behavior of the high-field $1/n_e e\rho_{xx}$ can thus be explained. At low temperatures elastic impurity scattering dominates and the low impurity density in these samples leads to very high mobilities in the absence of magnetic field. However, in high field where there is only one partly filled Landau level occupied, the density of states at the energy of any electron capable of scattering is enhanced and so the total scattering rate is increased dramatically, leading to the fall in $1/n_e e\rho_{xx}$.

As the temperature is increased the number of acoustic phonons increases, while at $B = 0$, the impurity scattering remains constant leading to a decrease in μ. The difference in high field is that while the increase in phonon number still tends to increase the scattering, this additional phonon scattering broadens the Landau levels which in turn reduces the density of states and so the elastic scattering will be less. The increase in Γ also reduces the phonon scattering through the requirement for self-consistency. This results in a range of temperature over which $1/n_e e\rho_{xx}$ either changes very little or shows a small increase. The size of this increase and the temperature at which its maximum occurs was seen to vary between the samples studied, which is not surprising as its origin is in the interaction of several terms. At high temperatures LO-phonon scattering becomes important but is not greatly affected by the magnetic field due to the large self-broadening of the LL's, so the magnetoresistance is reduced. As the magnetic field rises the increased importance of elastic scattering means that it is dominant up to much higher temperatures. For instance at 30 T the resistivity is not dominated by OPS until $T \sim 400$ K. Thus the scattering mechanisms usually only seen at very low temperature in the absence of magnetic field now continue to dominate ρ_{xx} up to high temperatures in strong magnetic fields.

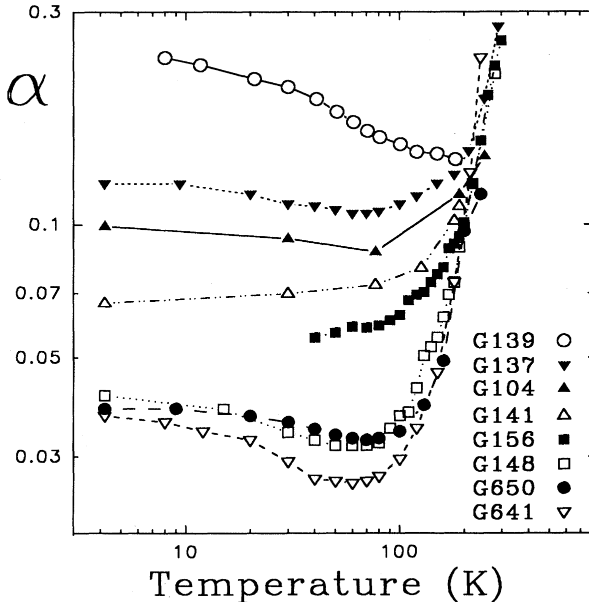

FIG. 5. Linear coefficient of resistivity α as a function of temperature for each sample (as indicated in the key), showing far from universal behavior. The lines are guides to the eye.

Figure 2 shows the effect of increasing the carrier density by photoexcitation. At low temperature, in the absence of field μ increases under photoexcitation for a number of reasons. The increased carrier concentration will increase the Fermi wave vector, and hence reduce the effect of scattering on momentum transfer. Higher n_e also increases the mobility through greater screening. Electron-hole pair creation in the GaAs has the effect of flattening the conduction band near the interface and reducing N_{depl} through trapping of electrons at acceptors, which will make b smaller (i.e., greater z extent of the wave function), but the increased n_e will tend to increase b. Since $\mu^0_{\text{IMP}} \propto n_e b^{-1}$ the change in b will determine whether the mobility increase is superlinear in n_e. However the phonon scattering in zero field is not as strongly affected by the electron concentration and so at higher temperatures the increase in μ from photoexcitation will be less.

In high magnetic field we have seen in Fig. 2 that after photoexcitation $1/n_e e\rho_{xx}$ remains constant at its enhanced value as the temperature is increased, until the electrons start to recombine with traps above 100 K. Inspection of Eqs. (33) for each scattering mechanism shows that the only effect of photoexcitation on Γ is through a change of b in the $\mathcal{W}_i$. The other effect of increasing n_e will be through the distribution function, but for both impurity and DPA scattering the form of $\mathcal{F}^0$ in Eq. (28) will be identical. Hence which elastic-scattering mechanism dominates the resistivity will be unimportant as regards the increase in $1/n_e e\rho_{xx}$ from the photoexcitation.

In general the agreement between experiment and theory is remarkably good. The only real discrepancy in detail is in the region of the maximum in $1/n_e e\rho_{xx}$ in the temperature range 60 K$< T <$150 K where the calculation tends to overestimate the increase for some samples. This suggests that the influence of the Landau-level broadening from phonon scattering on elastic scattering is slightly overstated in the calculations. This may be due to other factors that affect the mobility which have

been neglected such as band nonparabolicity and thermal population of higher electric subbands.

V. SUMMARY

In conclusion we have studied the high-field magnetoresistance in GaAs-$Ga_xAl_{1-x}As$ heterojunctions and found a satisfactory model to account for the temperature, magnetic-field, and electron-density dependence exhibited. The experiments show a quasilinear increase in resistance with increasing magnetic field. This is not predicted classically, but can be understood by considering the increase in density of states in each Landau level as the magnetic field increases.

As the temperature is increased from 4 K to 100 K the mobility in zero field falls rapidly, but in high magnetic field we have the surprising result that it remains virtually constant and may even increase around 80 K. The calculations based on the momentum balance equation explain this curious effect and indeed reproduce the experimental resistivity data over the whole temperature range both with and without magnetic field. The sample-dependent quantities required are the carrier concentration, the zero-field, zero-temperature limit of the mobility, determined by the impurity content of the sample, and γ, the ratio of momentum to energy relaxation times, determined by the fraction of remote and background impurities. This agreement is only possible when all the scattering processes are included self-consistently in calculating both the density of states and the resistivity.

At the lowest temperature the resistivity is dominated by elastic impurity scattering, but as the temperature increases so does the amount of phonon scattering. This reduces the mobility at $B = 0$ but in high magnetic field the increase in Landau-level width, due to the phonon scattering, reduces the amount of impurity scattering and so the total amount of scattering remains constant, as does the resistivity at fixed magnetic field. Eventually inelastic optic-phonon scattering takes over, although the temperature at which this occurs increases with magnetic field.

ACKNOWLEDGMENTS

The authors would like to thank R. Fletcher of Queen's University, Kingston, Canada for interesting discussions and assistance with this work during his visit to the Clarendon Laboratory. Part of this work was performed in the framework of Contract No. IT/SC/24 of the "Diensten voor progammatie van het Wetenschapsbeleid" (Belgium) and the "British-Flemish Academic Research Collaboration Programme." One of us (D.R.L.) would like to thank the Rutherford Appleton Laboratory for support during this project and one of us (F.M.P.) thanks the Belgian National Science Foundation.

* Permanent address: Department of Physics, Clarendon Laboratory, Parks Road, Oxford OX1 3PU, U.K.

[1] K. Hirakawa and H. Sakaki, Phys. Rev. B **33**, 8291 (1986).
[2] W. Walukiewicz, H.E. Ruda, J. Lagowski, and H.C. Gatos, Phys. Rev. B **30**, 4571 (1984).
[3] C.T. Foxon, J.J. Harris, D. Hilton, J. Hewett, and C. Roberts, Semicond. Sci. Technol. **4**, 582 (1989).
[4] T. Kawamura and S. Das Sarma, Phys. Rev. B **45**, 3612 (1992).
[5] G. Kido and N. Miura, J. Phys. Soc. Jpn. **52**, 1734 (1982).
[6] T. Rötger, G.J.C.L. Bruls, J.C. Maan, P. Wyder, K. Ploog, and G. Wiemann, Phys. Rev. Lett. **62**, 90 (1989).
[7] R.A. Smith, *Semiconductors* (Cambridge University Press, Cambridge, England, 1978), p. 104.
[8] D.R. Leadley, R.J. Nicholas, W. Xu, F.M. Peeters, J.T. Devreese, J.J. Harris, and C.T. Foxon, Physica B **184**, 197 (1993).
[9] See I. Gorczyca, T. Suski, E. Litwin-Staszewska, L. Dmowski, J. Krupski, and B. Etienne, Phys. Rev. B **46**, 4328 (1992), and references therein for a discussion of values of E_D.
[10] T. Ando, J. Phys. Soc. Jpn. **37**, 1233 (1974).
[11] A. Isihara and L. Smrčka, J. Phys. C **19**, 6777 (1986).
[12] P. Warmenbol, F.M. Peeters, and J.T. Devreese, Phys. Rev. B **37**, 4694 (1988).
[13] N. Mori, H. Murata, K. Taniguchi, and C. Hamaguchi, Phys. Rev. B **38**, 7622 (1988).
[14] D.R. Leadley, R.J. Nicholas, W. Xu, F.M. Peeters, J.T. Devreese, L. van Bockstal, F. Herlach, J. Singelton, J. Perenboom, J.J. Harris, and C.T. Foxon, Proceedings of the 10th International Conference on the Electronic Properties of Two-Dimensional Systems, Newport, 1993 [Surf. Sci. (to be published)].
[15] X.L. Lei and C.S. Ting, Phys. Rev. B **30**, 4809 (1984).
[16] W. Cai, X.L. Lei, and C.S. Ting, Phys. Rev. B **31**, 4070 (1985).
[17] K.K. Thornber and R.P. Feynman, Phys. Rev. B **1**, 4099 (1970); F.M. Peeters and J.T. Devreese, *ibid.* **23**, 1936 (1981).
[18] X.L. Lei, J.L. Birman, and C.S. Ting, J. Appl. Phys. **58**, 2270 (1985).
[19] D.R. Leadley, R.J. Nicholas, J.J. Harris, and C.T. Foxon, Semicond. Sci. Technol. **5**, 1081 (1990).
[20] B. Tanatar, M. Singh, and A.H. MacDonald, Phys. Rev. B **43**, 4308 (1991).
[21] F.F. Fang and W.E. Howard, Phys. Rev. Lett. **16**, 797 (1966).
[22] J.J. Harris, D.E. Lacklison, C.T. Foxon, F.M. Selten, A.M. Suckling, R.J. Nicholas, and K.W.J. Barnham, Semicond. Sci. Technol. **2**, 783 (1987).
[23] P.N. Argyres, Phys. Rev. B **39**, 2982 (1989); R.S. Fishman and G.D. Mahan, *ibid.* **39**, 2990 (1989); M. Huberman and G.V. Chester, Adv. Phys. **24**, 489 (1975); F.M. Peeters and J.T. Devreese, Phys. Status Solidi B **115**, 539 (1983).
[24] F.M. Peeters and J.T. Devreese, Solid State Phys. **30**, 81 (1984).
[25] G.D. Mahan, *Many-Particle Physics* (Plenum, New York, 1981), p. 166.